Desalination and Water Treatment
www.deswater.com

doi: 10.1080/19443994.2015.1098796

57 (2016) 22726–22733
October

Taylor & Francis
Taylor & Francis Group

Effects of nearshore evaporation rates on the design of seabed gallery intake systems for SWRO facilities located along the Red Sea shoreline of Saudi Arabia

Abdullah H.A. Dehwah[a], Khan Z. Jadoon[a], Samir Al-Mashharawi[a], Thomas M. Missimer[b,*]

[a]*Water Desalination and Reuse Center, King Abdullah University of Science and Technology, Thuwal 23955-6900l, Saudi Arabia*
[b]*U. A. Whitaker College of Engineering, Florida Gulf Coast University, 10501 FGCU Boulevard South, Fort Myers, Florida 33965-6565, USA, email: tmissimer@fgcu.edu*

Received 3 April 2015; Accepted 29 July 2015

ABSTRACT

Feed water to seawater reverse osmosis desalination systems should have a constant salinity with minimal variation. Intake systems that extract water from shallow nearshore areas in arid regions can exhibit significant fluctuations in salinity caused by high rates of evaporation and lack of circulation. Such fluctuations in salinity could inhibit the design, construction, and operation of seabed gallery intake systems located in shallow nearshore areas, such as the Red Sea inner shelf. Water depths range from 0 to 2 m between the beach and the edge of the fringing reef in the optimal locations for the development of seabed gallery intakes along the coast of the Red Sea of Saudi Arabia. The evaporation rate in this area is between 2 and 3 m per year. The bottom consists of mostly a marine hardground containing a thin veneer of unlithified sediment and no significant cover of corals or seagrass. The rather barren nature of the bottom suggests that periodic hypersalinity may contribute to the formation of hardgrounds on the bottom by causing supersaturation of the seawater with calcium carbonate and may limit the growth of corals and grasses. To assess the changes in salinity, a conceptual model was developed which assumes that a shallow circulation cell develops between the shoreline and deeper water offshore. Lower salinity seawater should migrate landward to replace water loss caused by evaporation with seaward moving of high-salinity water occurring along the bottom to balance the flow with ultimate mixing before the reef tract. To test this circulation pattern, a series of sensors were deployed to continuously monitor the water temperature, conductivity, and salinity at the surface and at the bottom during several periods of high air temperature. Surprisingly, the results show very little variation in salinity, despite the very high evaporation loss. The water salinity ranged between 39,000 and 40,000 mg/L with no diurnal variations of significance. Based on the monitoring and weather station data collected nearby, it appears that the predominant strong onshore wind, particularly during the afternoon and early evening, causes near-continuous mixing of the water between the reef tract and the shoreline. Therefore, the development of seabed gallery intake systems within the shallow water between 1 and 2 m of depth is feasible based on the measured salinity which is similar to that occurring further offshore in water depths between 2 and 20 m.

*Corresponding author.

Presented at EuroMed 2015: Desalination for Clean Water and Energy Palermo, Italy, 10–14 May 2015. Organized by the European Desalination Society.

1944-3994/1944-3986

Keywords: Seawater reverse osmosis; Seabed gallery intake; Nearshore circulation; Red Sea; Salinity variation

1. Introduction

It is an international goal to reduce the energy consumption and cost of seawater desalination to allow it to be used to provide water supplies to a greater number of people [1,2]. A significant component of this goal is to improve the quality of the raw seawater that is treated by the seawater reverse osmosis process (SWRO) [3]. One method of improving the quality of raw seawater that enters a SWRO facility is to utilize some type of subsurface intake system which provides a significant degree of pretreatment using natural filtration, similar to the bank filtration process used in freshwater river intakes in Europe and other regions for over a century [4]. Recent investigations have demonstrated that subsurface intakes provide a significant improvement in water quality by removing organic substances from the seawater, thereby decreasing the potential for biofouling of the SWRO membranes [5,6].

A considerable amount of research has been conducted on the use of subsurface intake systems along the Red Sea coast of Saudi Arabia [7–11]. The primary conclusion of this research is that the best type of subsurface intake that could be used to supply SWRO facilities of virtually any capacity is the offshore seabed gallery system. A number of site-specific investigations showed that the galleries could be constructed in the nearshore subtidal zone between the reef and the beach (Fig. 1).

A key assumption with regard to the technical feasibility of successfully operating a seabed gallery along coastline of the Red Sea is that the raw water salinity would remain the same as the background salinity with time, since this region is arid and has a high rate of free surface evaporation. A question has been raised concerning whether the shallow water near the shoreline becomes more saline during daily cycles caused by evaporative concentration. It is the purpose of this research to evaluate the nearshore changes in salinity on a diurnal basis to determine if the evaporative loss of seawater would cause a limitation to the use of seabed gallery intake systems in the nearshore areas of the Red Sea of Saudi Arabia.

2. Methods

The potential evapotranspiration for the nearshore of the Red Sea was calculated using the Penman method as applied to the weather station data collected near the shoreline at the King Abdullah University of Science and Technology. This station is representative of the general Red Sea region of Saudi Arabia, but some variation in data can be anticipated.

Conductivity and temperature data from the shallow nearshore water were collected at two sites: one located adjacent to the King Abdullah Economic City (KAEC) (site A) and another at a site adjacent to King Abdullah University of Science and Technology (KAUST) (site B) (Fig. 2).

Transducers were deployed into the field to measure the top and bottom conductivity and temperature at the two locations (site A, site B). The details of installation are shown in Fig. 3. Eight transducers were deployed at depths ranging from 0.6 up to 3.5 m below surface. Site A data were recorded continuously for a period of 7 weeks. Site B-1 data were recorded for a period of 4 weeks, while data were recorded for a one-week period only for site B-2 due to installation error.

Since wind is a key component of shallow nearshore circulation, wind data were collected from an onshore weather station located at King Abdullah University of Science and Technology. These data were compiled into a wind rose and were used to assess the potential for causing nearshore mixing of the water column.

3. Investigation results

3.1. Potential evaporation analysis

Hourly meteorological variables were recorded at a weather station installed on the coast of Red Sea near KAUST. The Penman method was used extensively to estimate potential evaporation (PE) and it requires air temperature, wind speed, relative humidity, and solar radiation data to perform this estimate. In this study, we used the energized Penman equation proposed by Van Bavel [12], which results in the below relationship:

$$E_p = \left[\frac{(L + K)[s(T_a)] + \rho_w \gamma K_e \lambda_v v_a [e_{sat}(T_a)](1 - W_a)}{\rho_w \lambda_v [e_{sat}(T_a) + \gamma]}\right] \times 100 \quad (1)$$

Fig. 1. Research sites on which investigations were conducted on seabed gallery feasibility.

where E_p is the evaporation rate (cm), the net radiation is represented by $(L + K)$ in which L is the net long wave radiation (MJ m^{-2}), and K is the net incoming short wave radiation (MJ m^{-2}), and the slope of the saturation vapor pressure (kPa ℃ $^{-1}$) is s(T_a) at the surface temperature. The density of water (kg m^{-3}) is ρ_w and γ corresponds to the psychrometric constant (kPa ℃ $^{-1}$). The mass transfer is defined by K_e (kPa^{-1}) and λ_v corresponds to the latent heat of vaporization (MJ kg^{-1}). e_{sat} is the saturation vapor pressure (kPa) and v_a is the velocity of air (m/s). The relative humidity is denoted by W_a in the equation.

Fig. 4(a) and (b) depicts the hourly and monthly PE estimated over a period of one year. Zero day of the year corresponds to the first day of the year. The increasing trend of PE was observed in the first 150 d of the year and a maximum PE rate of 0.17 cm/h was estimated. Monthly PE shows a similar trend and a maximum monthly PE of 29.2 cm/month was observed in May. The ambient temperature decrease in the winter causes the PE to decrease and this can be observed especially after the month of September. In a year, 262.28 cm PE was observed near the coast of Red Sea.

3.2. Conductivity and temperature data

For both sites, there was a clear positive relation between temperature and conductivity measurements as shown in Fig. 5(a) and (b). At both sites, the conductivity values were in correspondence with temperature measurements. The measurements of top and bottom points were almost equal at both sites with no clear difference observed based on the depth change. The conductivity measurements were in the range of 56 and 62 mS/cm during the deployment period, while the temperature was in the range of 23 and 28℃. In order to clearly understand the temperature effect on electrical conductivity (EC), a temperature-standardized equation was used in which EC values were standardized at a reference temperature of 25℃:

$$EC_{25} = EC_a \times \left[0.4470 + 1.4034 \times (e)^{\left(\frac{T}{26.815}\right)}\right] \quad (2)$$

where EC_{25} is the standardized EC_a and T is the water temperature in ℃ [13].

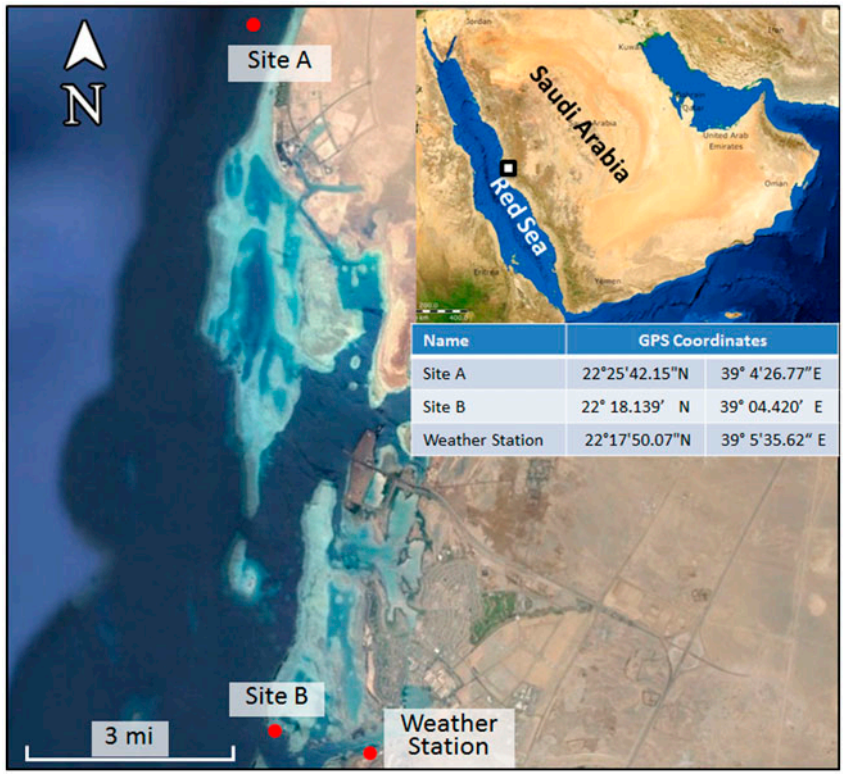

Fig. 2. Location of the two deployment sites and the weather station.

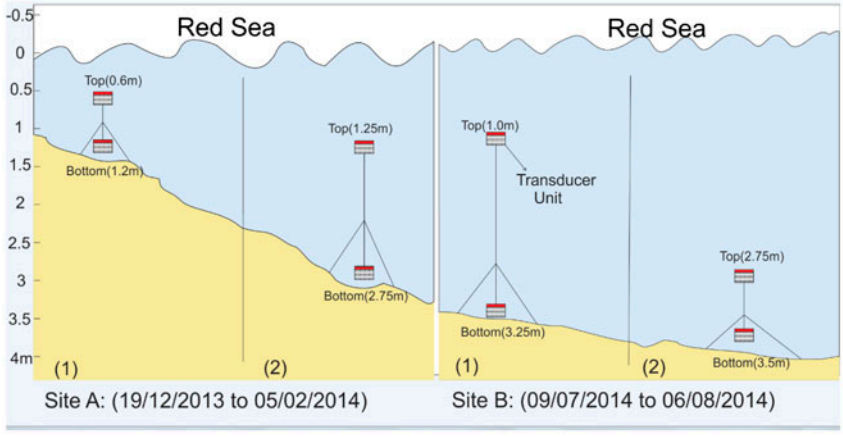

Fig. 3. Deployment of transducer units.

In order to identify the role of water depth in conductivity and temperature change, the standardized measurements of EC from site A are plotted in Fig. 6.

The standardized conductivity measurements for site B are shown in Fig. 7.

3.3. Wind data diagram

Fig. 8 shows the wind rose diagram based on one year of hourly wind data recorded by weather station installed at the coast near KAUST. This rose shows that the winds on the coast blow from the northwest most of the time, which is an onshore direction. The wind speed was recorded in meters per second and the legend at the right bottom corner shows the wind speed categories and their associated colors. The six spokes around the northwest direction comprise 34% of all hourly wind directions. The wind rarely blows from the southwest or the northeast. The wind rose diagram also provides details on speeds from different

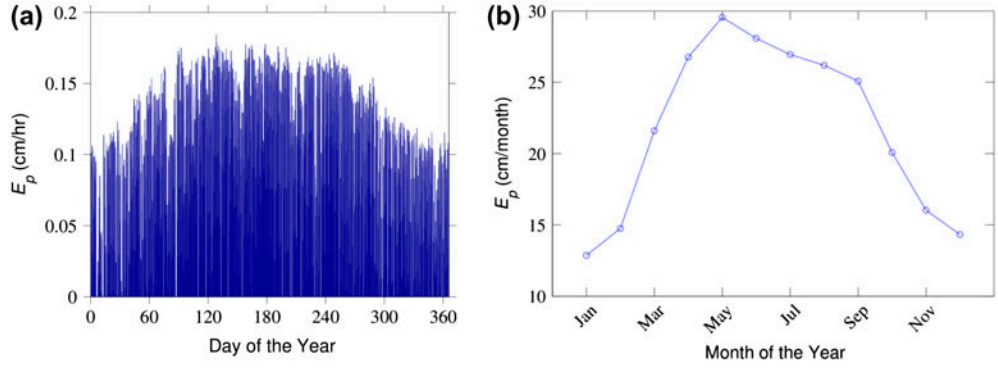

Fig. 4. (a) Hourly potential evaporation flux estimated over 365 d of a year and (b) monthly potential evaporation values estimated by Penman equation.

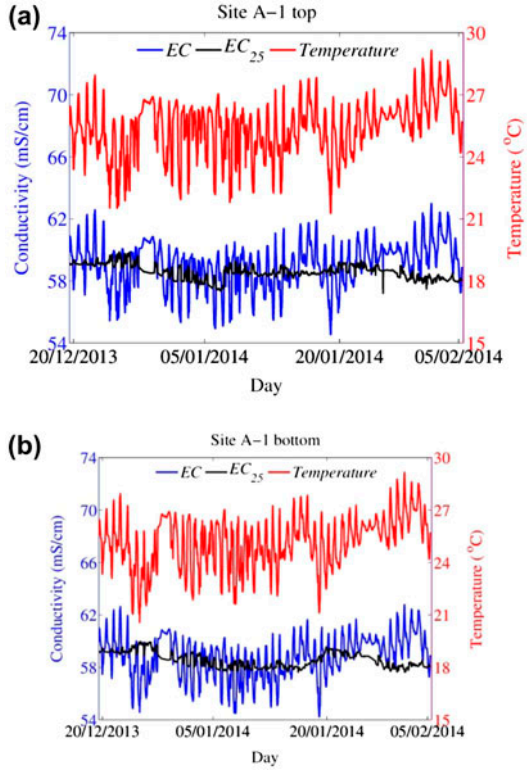

Fig. 5. EC and temperature measurements for site A-1 top (a) and for site A-1 bottom (b). The standardized EC is shown in black.

directions. Examining winds from the northwest (the longest spoke), one can determine that approximately 3% of the time, the wind blows from the northwest at speeds between 4 and 6 m per second. Similarly, on this spoke, it can be calculated that winds blow from the northwest at speeds between 6 and 8 m/s about 2.8% of the time (5.8–3%), at speeds between 8 and 10 m/s about 1.2% of the time, and between 10 and 12 m/s about 0.3% of time.

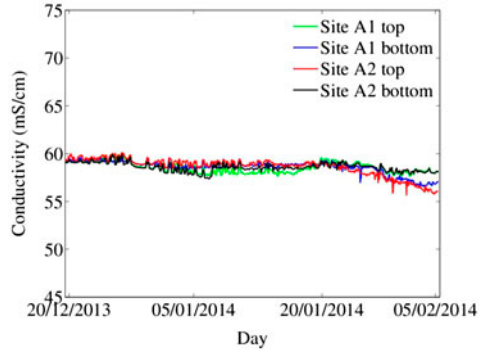

Fig. 6. Standardized conductivity measurements for site A.

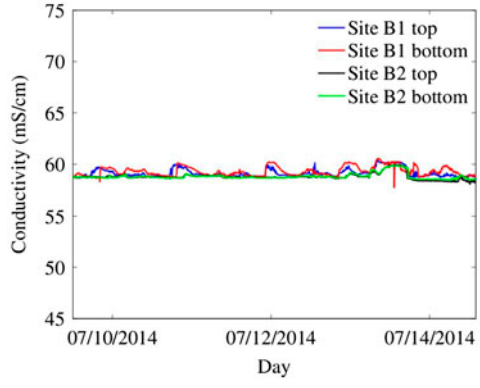

Fig. 7. Standardized conductivity measurements for site B.

4. Discussion

Thermohaline circulation is a common process of deep ocean circulation which controls the overall movement of large water masses [14,15]. Perhaps, similar thermohaline cells of a very small size can form in shallow, nearshore areas where there is a very high

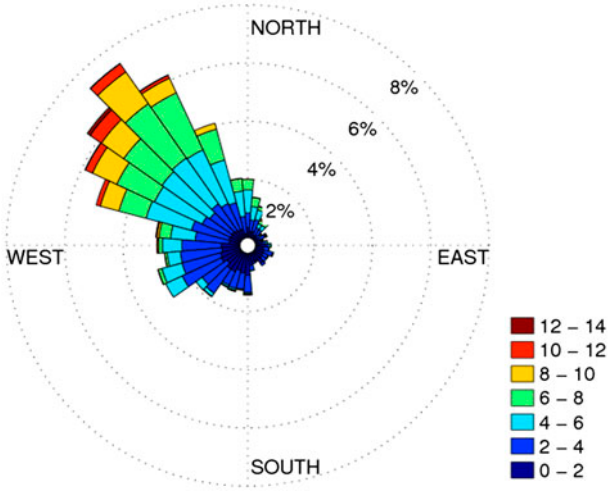

Fig. 8. Wind data at KAUST weather station, values are given in (m/s).

rate of free surface evaporation and wind-driven wave action is minimal. In these shallow areas, the seawater would be evaporatively concentrated at the surface, sink to the bottom, and move seaward with the bottom slope. Fresher seawater would move landward to balance the mass of water lost through evaporation and the seaward moving density current (Fig. 9). This nearshore circulation would have the tendency to cause the occurrence of hardgrounds and the absence of marine flora and fauna that are sensitive to high-salinity water. This is the observed condition of a large portion of the nearshore area of the Arabian Sea of Saudi Arabia.

It has been demonstrated that thermally driven exchanges occur between a coral reef and the adjacent ocean at the northern end of the Gulf of Aqaba [16]. The heating of shallow water causes an offshore movement of water at the surface and a balancing onshore flow of water at depth. This is an opposing flow cell compared to potential seaward-directed bottom flow caused by density. Wind-driven nearshore circulation in coral reef systems is known to facilitate circulation within reef and lagoon systems [17–19].

The occurrence of higher salinity bottom water during the summer months or during part of the diurnal cycle would be of great concern in the event that a seabed gallery intake was to be used to provide feedwater for a SWRO facility. The salinity of the nearshore water in the Red Sea is commonly between 40 and 42 ppt and any increase would provide difficulties to the operation of the facility.

An analysis of the PE of the nearshore of the Red Sea shows that the total annual PE ranges from 2 to 3 m. The highest daily rates would occur during the day in the summer months. The calculated PE data appear to support the potential for allowing thermohaline circulation to occur during part of the year within the nearshore zone.

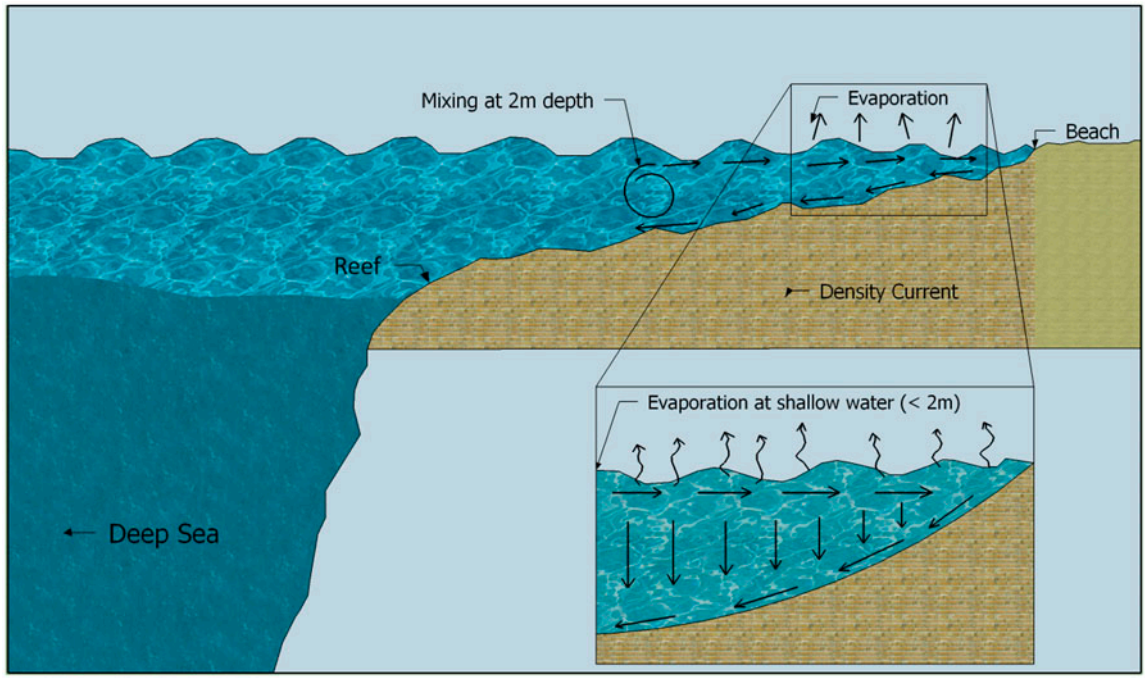

Fig. 9. Theoretical density circulation in the nearshore shallow area of the Red Sea based on evaporation.

The monitoring of the shallow water during part of the year at site A and site B showed that no significant salinity and temperature gradients are formed in the shallow nearshore area. The likely reasons for mixing in this area are: (1) the water depth may be too shallow to accommodate density current formation, (2) the bottom slope is insufficient to allow a density current to form, and (3) the strong onshore wind causes sufficient nearshore circulation to prevent the formation of vertical density gradients, nearshore density circulation, and wave-driven shallow circulation. Based on the data observed from the site along the Red Sea shoreline, it is likely that a combination of wind- and wave-driven circulation causes mixing and convection with nearshore outer and inner reef areas as described in locations of the Red Sea and other regions [20–22].

While this research is specific to the Red Sea coast of Saudi Arabia, the nearshore circulation could affect salinity changes at other geographic sites where seabed gallery intakes may be considered for installation. For example, the circulation of the Arabian Gulf is affected by an offshore wind direction along the Saudi Arabian coast and other locations where high salinity in shallow water is documented. Therefore, evaporative concentration of salinity could be a significant problem [23]. The coastlines of the Mediterranean tend to have a larger variation in wind direction and intensity, so site-specific investigations of nearshore circulation would be required during the intake design process in this locality.

5. Conclusions

An investigation of variations in nearshore salinity and temperature was conducted to ascertain the potential for the formation of high-salinity bottom water along the Red Sea nearshore area of Saudi Arabia. The formation of a high-salinity water mass and seaward circulation could adversely affect the operation of a seabed gallery intake by causing a fluctuation of the intake water salinity which would influence plant operations. The investigation showed that no such vertical density gradient was formed and no significant shallow thermohaline circulation was occurring. It is likely that the absence of a vertical density gradient and formation of circulation are caused by wind mixing and the low degree of seaward-dipping bottom slope.

While the results of this investigation are positive with regard to the viability of using seabed gallery systems constructed in shallow, nearshore water of the Red Sea of Saudi Arabia, care still must be taken to map the bottom bathymetry to be sure that slope allows free movement of water. The presence of a shallow basin could allow high-density water to accumulate within it and limit the impacts of mixing processes on the water column.

Acknowledgments

This research was funded by the Water Desalination and Reuse Center and baseline research funding was provided by the King Abdullah University of Science and Technology. The authors would like to thank Coastal and Marine Resources Core Lab and the Red Sea Center for providing equipment for conductivity, temperature measurements, and the vessel as well as for providing access to weather station data.

References

[1] World Bank, Making the Most of Scarcity: Accountability for Better Water Management in the Middle East, World Bank, Riyadh, Kingdom of Saudi Arabia, 2010.
[2] N. Ghaffour, T.M. Missimer, G.L. Amy, Technical review and evaluation of the economics of water desalination: Current and future challenges for better water supply sustainability, Desalination 309 (2013) 197–207.
[3] T.M. Missimer, Water Supply Development for Membrane Water Treatment, Aquifer Storage, and Concentrate Disposal for Membrane Water Treatment Facilities, Schlumberger Water Services, Sugar Land, Texas, second ed., 2009, p. 390.
[4] T.M. Missimer, N. Ghaffour, A.H.A. Dehwah, R. Rachman, R.G. Maliva, G. Amy, Subsurface intakes for seawater reverse osmosis facilities: Capacity limitation, water quality improvement, and economics, Desalination 322 (2013) 37–51.
[5] R.M. Rachman, S. Li, T.M. Missimer, SWRO feed water quality improvement using subsurface intakes in Oman, Spain, Turks and Caicos Islands, and Saudi Arabia, Desalination 351 (2014) 88–100.
[6] A.H.A. Dehwah, S. Li, S. Al-Mashharawi, H. Winters, T.M. Missimer, Changes in feedwater organic matter concentrations based on intake type and pretreatment processes at SWRO facilities, Red Sea, Saudi Arabia, Desalination 360 (2015) 19–27.
[7] A.H.A. Dehwah, S. Al-Mashharawi, T.M. Missimer, Mapping to assess feasibility of using subsurface intakes for SWRO, Red Sea coast of Saudi Arabia, Desalin. Water Treat. 52 (2013) 2351–2361.
[8] K. Sesler, T.M. Missimer, Technical feasibility of using seabed galleries for seawater RO facility intakes and pretreatment: Om Al Misk Island site, Red Sea, Saudi Arabia, IDA J. Desalin. Water Reuse 4(4) (2012) 42–48.
[9] A.H.A. Dehwah, T.M. Missimer, Technical feasibility of using gallery intakes for seawater RO facilities, northern Red Sea coast of Saudi Arabia: the King Abdullah Economic City site, Desalin. Water Treat. 51 (34–36) (2013) 6472–6481.

[10] D. Mantilla, T.M. Missimer, Seabed gallery intake technical feasibility for SWRO facilities at Shuqaiq, Saudi Arabia, J. Appl. Water Eng. Res. 2(1) (2014) 3–12, doi: 10.1080/23249676.2014.895686.
[11] S. Al-Mashharawi, A.H.A. Dehwah, K.B. Bandar, T.M. Missimer, Feasibility of using a subsurface intake for SWRO facility south of Jeddah, Saudi Arabia, Desalin Water Treat. 55(13) (2015) 3527–3537.
[12] C.H.M. Van Bavel, Potential evaporation: The combination concept and its experimental verification, Water Resour. Res. 2(3) (1966) 455–467.
[13] K.R. Sheets, J.M.H. Hendrickx, Noninvasive soil water content measurement using electromagnetic induction, Water Resour. Res. 31(10) (1995) 2401–2409, doi: 10.1029/95WR01949.
[14] W.S. Broeker, The great ocean conveyor, Oceanography 4 (1991) 79–89.
[15] M. Cox, An idealized model of the World ocean. Part I: The global-scale water masses, J. Phys. Oceanogr. 19 (1989) 1730–1752.
[16] S.G. Monismith, A. Genin, M.A. Reidenbach, G. Yahel, J.R. Koseff, Thermally Driven exchanges between a coral reef and the adjoining ocean, J. Phys. Oceanogr. 36 (2006) 1332–1347.
[17] H.B. Fischer, E.J. List. R.C.Y. Koh, J. Imberger, Mixing in Inland and Coastal Waters, Academic Press, New York, 483.
[18] S.B. Kraines, T. Yanagi, M. Isobe, H. Komiyama, Wind-wave driven circulation on the coral reef at Bora Bay, Miyako Island, Coral Reefs 17 (1998) 133–143.
[19] T. Berman, N. Paldor, S. Brenner, Simulation of wind-driven circulation in the Gulf of Elat (Aqaba), J. Mar. Syst. 26 (2000) 349–365.
[20] H.H. Roberts, S.P. Murray, J.H. Suhayda, Physical processes in a fringing reef system, J. Mar. Res. 33 (1975) 233–260.
[21] A. Wolf-Vecht, N. Paldor, S. Brenner, Hydrographic indications of advection/convection effects in the Gulf of Elat, Deep Sea Res. Part A. Oceanogr. Res. Pap. 39 (1992) 1393–1401.
[22] G. Symonds, K.P. Black, I.R. Young, Wave-driven flow over shallow reefs, J. Geophys. Res. 100 (1994) 2639–2648.
[23] R. Rachman, T.M. Missimer, Technical feasibility for development of a seabed gallery intake for SWRO at Abu Ali, Arabian Gulf, Saudi Arabia, Desalin. Water Treat. 53(13) (2015) 3538–3546.